

# Vibration Control of a Cantilever Beam Using a Tunable Vibration Absorber Embedded with ER Fluids

Chih-Jer Lin, Chun-Ying Lee, Chiang-Ho Cheng, and Geng-Fung Chen

**Abstract**—This paper investigates experimental studies on vibration suppression for a cantilever beam using an Electro-Rheological (ER) sandwich shock absorber. ER fluid (ERF) is a class of smart materials that can undergo significant reversible changes immediately in its rheological and mechanical properties under the influence of an applied electric field. Firstly, an ER sandwich beam is fabricated by inserting a starch-based ERF into a hollow composite beam. At the same time, experimental investigations are focused on the frequency response of the ERF sandwich beam. Second, the ERF sandwich beam is attached to a cantilever beam to become as a shock absorber. Finally, a fuzzy semi-active vibration control is designed to suppress the vibration of the cantilever beam via the ERF sandwich shock absorber. To check the consistency of the proposed fuzzy controller, the real-time implementation validated the performance of the controller.

**Keywords**—Electro-Rheological Fluid, Semi-active vibration control, shock absorber, fuzzy control, Real-time control.

## I. INTRODUCTION

RECENTLY, smart materials have been inspired and designed in living applications, such as shape memory alloys (SMA), piezo-electrical ceramics, magnetic-rheological fluids (MRF) and electro-rheological fluids (ERF). Smart materials have applied in vibration control problems due to their varied physical phenomena such as piezoelectric effect, magnetic-rheological and electro-rheological properties. ER fluids are suspensions of extremely fine non-conducting particles in an electrically insulating fluid. The apparent viscosity of ERFs changes reversibly in response to an electric field. A typical ERF can change from a liquid to a gel with response times of milliseconds. This effect was discovered and first reported by Willis Winslow, who obtained a US patent on the effect in 1947 and wrote an article published in 1949[1]. Therefore, the effect is sometimes called the Winslow effect. Since the discovery of ERF by Winslow in 1940's, ERF have drawn many studies on the theoretical modeling and applications, because ERF has significant reversible changes in

damping and stiffness under the influence of an applied electric field.

ERFs can quickly respond in enhancement of apparent viscosity by as high as five orders in response to an applied electric field. When a very high electric field is applied to the ERF, it will change from a Newton fluid to a forming chain-like structure, which is called a Bingham plastic. The Bingham plastic is a viscoplastic material that behaves as a rigid body at low stresses but flows as a viscous fluid at high stress. However, when the applied electric field is removed, the ERF behaves as a Newton fluid with response times of milliseconds. These reversible and controllable rheological properties of ERFs make them attractive for applications in devices such as clutches, valves, shock absorbers, and vibration dampers [2].

Many researchers have studied active or semi-active vibration control of structure using the ER fluids based on various control strategies. Gandhi and Thompson proposed the application of ER fluids to achieve the vibration control of the adaptive structures [3]. Choi et al. derived an empirical model for predicting the vibration characteristics responding to electrical field and studied the vibration properties for hollow cantilevered beams filled with ER fluids [4]. Yalcintaset al. investigated the semi-active control of ER adaptive beams and illustrated the capabilities theoretically and experimentally [5]. Choi et al. investigated the active vibration control and the active vibration characteristics of hollow cantilevered beams embedded with ER fluids [6]. Rahn and Joshi designed a feedback control system to control the vibration of the cantilevered ER beam [7]. Wei et al. investigated the feasibility of applying ER fluids to the vibration control of rotating flexible beams [8].

However, the ER materials in the above-mentioned literatures were not used for the applications for dynamic vibration absorbers. After Frahm first invented the dynamic vibration absorber in 1911 [9], there have been many researches in the development of the tuned vibration absorber (TVA) for various applications [10], [11]. Generally speaking, a tunable TVA is to incorporate the structure with a variable stiffness element in the absorber. Several materials with controllable stiffness properties have been proposed, such as: viscoelastic solid, shape memory alloys, piezoelectric materials, ER fluids, magnetorheological (MR) fluids and elastomers. The mechanisms of the variable stiffness can be achieved via adjustment in the material properties or the change in geometry or shape [12], [13]. The stiffness of a sandwich beam embedded with ER fluids can be easily varied and controlled; hence, it is very suitable for the semi-active vibration control as a

Chih-Jer Lin and Geng-Fung Chen are with Graduate Institute of Automation Technology, National Taipei University of Technology, Taipei 10608, Taiwan (886-2-2771-2171 ext. 4328; fax: 886-2-2711-1401; e-mail: cjlin@ntut.edu.tw).

Chun-Ying Lee is with the Department of Mechanical Engineering, National Taipei University of Technology, Taipei 10608, Taiwan (e-mail: leech@ntut.edu.tw).

Chiang-Ho Cheng is with the Department of Mechanical and Automation Engineering, University of Dayeh, Dacun, Changhua, Taiwan (e-mail: chcheng@mail.dyu.edu.tw).

TVA. Compared with the activecontrol counterparts, the TVA using ER fluids provides simpler design and is more power efficient in high level of excitation. With the applied electric field, ER fluids change from Newtonian flow to Bingham plastic. The electric field makes the suspended particles polarized and connected with each other to form chain. As electric field is applied, the viscosity and the yield stress of the ER fluid increases. Therefore, the main objective of this article is to present the achievements of controlling a sandwich beam embedded with ER fluid as a TVA.

This paper is organized as follows. Section II presents the fabrication of the ERF sandwich beam and its frequency response is measured to establish the characteristics' database for a vibration absorber. Section III describes the semi-active control architecture using the ERF TVA to suppress the vibration of a cantilevered beam structure. Based on the experimental results, a fuzzy controller is proposed to accomplish the semi-active vibration control using the TVA. To check the consistency of the proposed fuzzy controller, the real-time implementation is performed to validate the proposed controller. Section IV describes the real-time experimental investigations using NI compact RIO. Finally, Section V draws conclusions.

## II. THE SYSTEM SETUP

### A. Fabrication of ER Sandwich Beam

Fig. 1 describes a schematic diagram of a sandwich beam embedded with ER fluid. The ER fluid consists of two components: corn starch and silicon oil (KF-96-20cs), where the weight fraction of the corn-starch suspensions is almost 45%~50%. The carrier fluid, produced by Shin Etsu Corp., has a viscosity of 20 cs. On one hand, the top and bottom plates of sandwich beam are made of aluminum with the thickness of 0.3mm and the edges are made of rubber. Therefore, the ER fluid is confined on the rubber dam and aluminum plates. On the other hand, the two aluminum plates also act as the electrodes of the applied electrical field. An acrylic pad is used as the rigidity for the clamped side, which can be connected to the other structure. The dimensions and the specifications of the ERF TVA are described in Table I.

### B. Measurement of the ER Sandwich Beam's Characteristics

Fig. 2 depicts a schematic diagram of the experimental setup for measuring the dynamic characteristics of the ER beam specimen of Fig. 1. An electromagnetic vibration shaker (LDS PA500L) provides the exciting force to the clamped side of the ER beam and a high-voltage power amplifier is connected to the electrodes of the aluminum face-plates to provide the required electric field during the test. To analyze the dynamic characteristics of the ER beam at the different applied electric fields, a dynamic signal analyzer (HP 35665A) is used to process the analog signals from the eddy-current probe. In the experiments, the electromagnetic actuator provided an actuating signal in the form of a swept sine wave at the frequency from 0 to 200 Hz on the ER beam to measure the transverse vibration response at the free end. The accelerometer (PCB 333B32) is

used to measure the acceleration of the input excitation and a non-contacting eddy-current displacement probe (Keyence AH-416) is used to measure the deflection of the ER beam's free end. The input and output measured time response signals were fed to the dynamic signal analyzer and Fig. 3 shows the frequency response obtained using fast Fourier transform (FFT). The same experimental steps were repeated at varying electrical field from 0 to 2 (kV/mm) in 0.25 (kV/mm) increments. Fig. 3 shows the relationship between the frequency response and the corresponding electric field of the ER sandwich beam. The peak values of each curve represent the natural frequencies of the ER sandwich beam and Fig. 4 illustrates the effect of electric field strength on the first two modes' frequencies of the proposed beam. It is shown that the natural frequencies of the each mode increase as the strength of the applied electrical field increases. The high electric field makes the ERF change from a Newton fluid to a Bingham plastic so that the stiffness of ER sandwich beam is increased. Based on the results in Figs. 3, 4, the vibration characteristics of ER beam could be controlled by changing the strength of the applied electric field. Therefore, the ER sandwich beam with controllable stiffness can be used as a TVA to incorporate with a main structure to suppress vibration.

TABLE I  
 THE SPECIFICATIONS OF THE ERF SANDWICH BEAM

| L                            | W     | $h_1$   | $w_1$  | $h_2$                        |
|------------------------------|-------|---------|--------|------------------------------|
| 150 mm                       | 30 mm | 0.3 mm  | 2.5 mm | 2 mm                         |
| Adhesives                    | ERF%  | Volume  | Weight | Equivalent density           |
| Hi-temp.<br>Silicone Sealant | 45%   | 7.25 mL | 28.6 g | 2118.52<br>kg/m <sup>3</sup> |

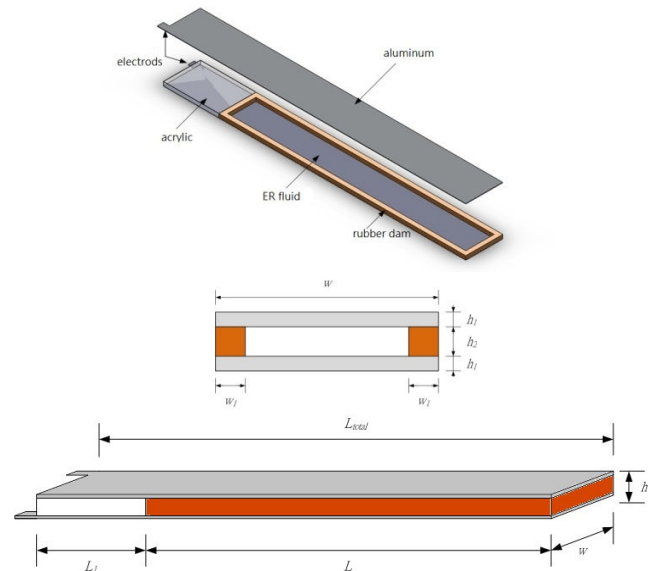


Fig. 1 The structure diagram and dimension of the ER sandwich beam

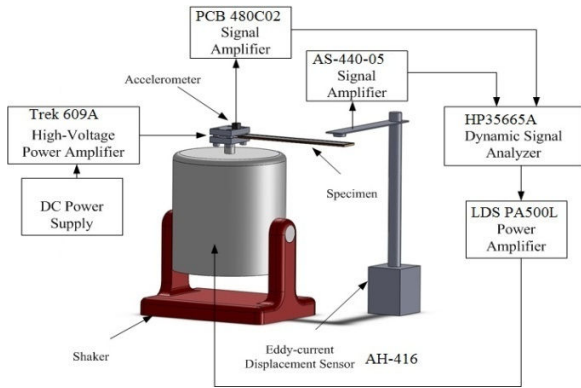


Fig. 2 Schematic diagram of the experimental setup for measuring the dynamic characteristics of the ER sandwich beam

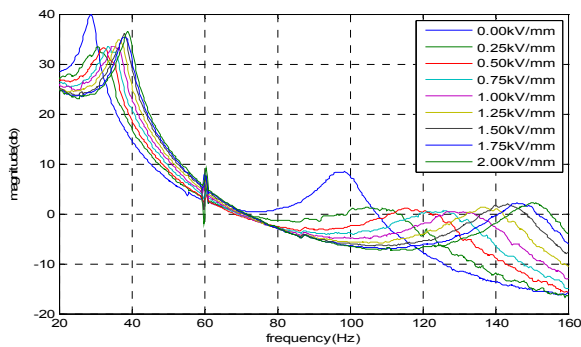


Fig. 3 The relationship between the frequency response and the corresponding electric field of the ER sandwich beam

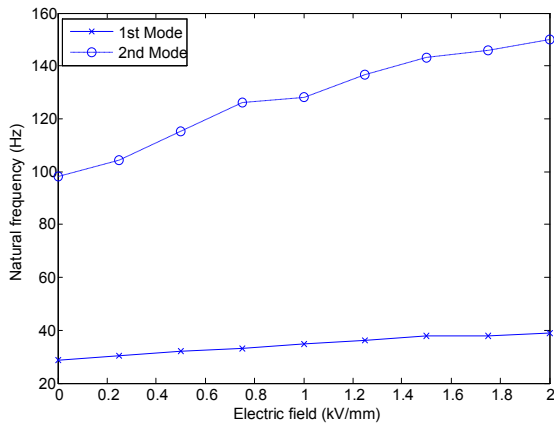


Fig. 4 Effect of electric field on the ER sandwich beam

### III. FUZZY SEMI-ACTIVE CONTROLLER DESIGN

To determine the optimal parameters for the vibration control, numerous studies have been phenomenologically performed to understand that the stiffness and energy dissipation characteristics of the ERF beam with respect to the applied electric field. Based on the field-dependent frequency responses in Fig. 3, the optimal applied electric field can be designed to follow a selection of minimizing the envelopes of the amplitude at excitation frequency bandwidths. Choi and Park derived the

fuzzy controller for attenuating the undesired vibration for the ERF cantilevered beam based on the frequency-dependent control strategy [6]. Therefore, the switching algorithm of the controlled electric field can be designed according to the mapping between the frequency response and the applied electric field as shown in Fig 3. To implement the ERF sandwich beam as a TVA for a vibration control of the structure, the fuzzy controllers for semi-active vibration control are discussed as follows.

#### A. Vibration Control Design Using the ER Sandwich TVA

Fig. 5 shows a proposed schematic diagram of semi-active vibration control architecture for a structure using the ER sandwich TVA. The main structure is an aluminum beam, whose length is 80mm, width is 30mm and thickness is 2 mm. At the free end of the main structure, an acrylic flexure is used to clamp the ER sandwich beam with the main structure. The accelerometer (PCB 333B32) is used to measure the acceleration of the main structure at the free end and this signal is fed back to the real-time controller (cRIO-9074), which is used to accomplish the proposed fuzzy controllers, and then the control signal is amplified by the high-voltage power amplifier (Trek 609A) to produce the desired electric field to the ERF. The dynamic signal analyzer (HP 35665A) is used to capture the signal from the eddy-current probe to compare the time responses the open loop system with the closed loop system with the proposed vibration controller.

After the ER Sandwich TVA is connected to the main structure, the electromagnetic actuator is used to actuate in the form of a swept sine wave at the frequency from 0 to 200 Hz on the main structure to measure the transverse vibration response at the main structure's free end for the applied electric field from 0 to 2kV/mm on the ERF TVA. Fig. 6 shows the relationship between the frequency response (for the 1<sup>st</sup> mode) and the corresponding electric field (0~2 kV/mm). As shown in Fig. 6, the first resonant frequency of the whole system is about 18.5 Hz as there is no applied electric field and its first resonant frequency change to 21Hz as the applied electric field is 2 kV/mm.

For the first mode, the amplitude of the resonant frequency decreases as the applied electric field increases. Therefore, using the half-power point method can obtain the relation between the damping ratio of the whole system and the corresponding applied electric field can as shown in Fig. 7. From the results in Fig. 7, the damping ratio increases as the applied electric field increases from 0 to 1kV/mm and then it appears saturation as the applied electric field is larger than 1kV/mm. Based on the above experimental results, the ERF TVA can be controlled to make the resonant frequency and amplitude varied according to the applied electric field. Therefore, the next step is to design a fuzzy controller to implement the semi-active control.

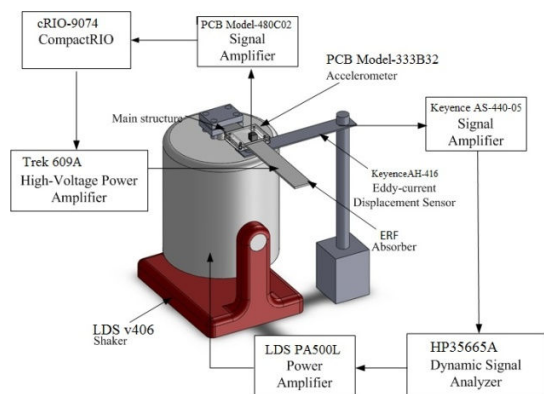


Fig. 5 Schematic diagram of semi-active vibration control architecture for a structure using the ER sandwich TVA

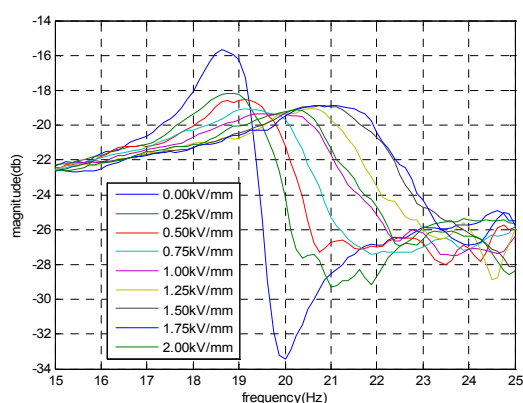


Fig. 6 The relationship between the frequency response (for the 1<sup>st</sup> mode) and the corresponding electric field (0~2 kV/mm)

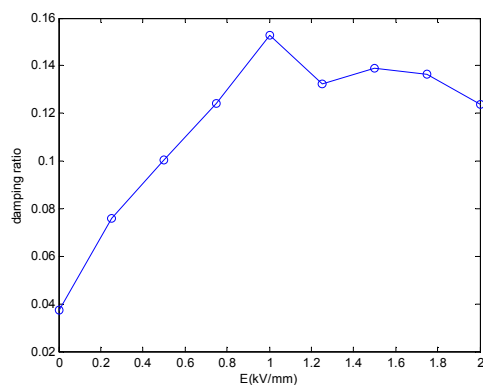


Fig. 7 The relation between the damping ratio of the whole system and the corresponding applied electric field

### B. Fuzzy Controller Design

The block diagram of vibration control system using ERF is shown in Fig. 5. It can be considered as a semi-active control system where the ERF electric field is the output of the controller and the acceleration of the structure's vibration accelerometer is fed back to the controller. The accelerometer (PCB 333B32) is used to measure the acceleration of the main structure at the free end and this signal is fed back to the real-time controller (cRIO-9074), which is used to accomplish the proposed fuzzy controllers, and then the control signal is amplified by the

high-voltage power amplifier (Trek 609A) to produce the desired electric field to the ERF.

To establish the rule base for the fuzzy controller, the experimental results with different frequencies and various amplitudes should be tested and measured at first. Under the different applied electric field of the ERF, the excitation with the specified amplitudes and the frequencies (10, 15, 20, 25, 30, 35, 40, 50, 60 Hz) are applied to the main structure. Tables II and III show the experimental results for the excitation's frequency at 10, 15, 20 and 30 (Hz) where each column shows the results at the different input voltage to the shock amplifier (50~200mVpk) and each row shows the results under the different electric field. In these tables, the bold fonts represent the optimal choice at the specified excitation, because the root-mean-square (RMS) value of the acceleration for the main structure is minimized. The RMS value of the acceleration is obtained as follows.

$$a_{rms} = \sqrt{\frac{1}{T} \int_{T_1}^{T_2} a^2 dt} \quad (1)$$

where  $a_{rms}$  is the root-mean-square value (RMS) of the acceleration,  $T_1$  and  $T_2$  are the initial and final time, and  $TT=T_2-T_1$ .

The relation between the damping ratio and the applied electric field is nonlinear as shown in Fig. 7 so that the above experimental results can provide the information about how to establish the fuzzy rules for the fuzzy controller. To build the mapping between the excitation and the optimal electric field to the ERF TVA, a novel semi-active fuzzy controller is proposed with two inputs and one output as shown in Fig. 8. For the proposed fuzzy controller, the first input is the RMS value of the acceleration provides the information about the amplitude of the vibration; the second input is the vibration frequency, which can be obtained by the FFT of the acceleration.

TABLE II  
 THE EXPERIMENTAL RESULTS FOR THE EXCITATIONS AT 10 AND 15 Hz

| Accelerator (mV) | Excitation at 10Hz |             |             |             | Excitation at 15Hz |             |             |             |
|------------------|--------------------|-------------|-------------|-------------|--------------------|-------------|-------------|-------------|
|                  | Shocker input (mV) |             |             |             | Shocker input (mV) |             |             |             |
|                  | 50                 | 100         | 150         | 200         | 50                 | 100         | 150         | 200         |
| 0                | 4.5                | 11.2        | 18.8        | 23.3        | 8.9                | 18.4        | 26.2        | 35.6        |
| 0.3              | 4.6                | 9.9         | 15.0        | 20.6        | <b>8.4</b>         | <b>17.8</b> | <b>25.7</b> | <b>34.7</b> |
| 0.5              | 4.2                | 9.5         | <b>13.4</b> | 18.4        | 10                 | 18.6        | 26.3        | 35.2        |
| 1                | 4.4                | <b>9.32</b> | 14.3        | 19.2        | 13                 | 22.3        | 29.1        | 37.3        |
| 1.5              | <b>4.2</b>         | 9.3         | 13.7        | 19.3        | 12                 | 23.9        | 31.4        | 39.2        |
| 2                | 4.2                | 9.38        | 14.2        | <b>18.4</b> | 12                 | 23.5        | 30.8        | 38.1        |

TABLE III

THE EXPERIMENTAL RESULTS FOR THE EXCITATIONS AT 20 AND 30HZ

| Acceler-<br>ation<br>(mV) | Excitation at 20Hz |             |             |             | Excitation at 30Hz |             |            |            |
|---------------------------|--------------------|-------------|-------------|-------------|--------------------|-------------|------------|------------|
|                           | Shocker input (mV) |             |             |             | Shocker input (mV) |             |            |            |
|                           | 50                 | 100         | 150         | 200         | 50                 | 100         | 150        | 200        |
| 0                         | <b>18</b>          | 39.0        | 55.2        | 72.3        | 46.9               | 97.6        | 149        | 201        |
| 0.3                       | 18.2               | 37.9        | 54.6        | 72.4        | 45.6               | 97.5        | 148        | 200        |
| 0.5                       | 18.3               | <b>32.2</b> | <b>48.6</b> | <b>65.3</b> | 42.7               | 95.0        | 147        | 198        |
| 1                         | 19.5               | 32.8        | 49.2        | 68.2        | 40.2               | 91.2        | 142        | 195        |
| 1.5                       | 19.9               | 37.7        | 54.7        | 71.9        | 39.3               | <b>89.3</b> | 142        | 193        |
| 2                         | 18.5               | 35.2        | 51.5        | 67.7        | <b>39.2</b>        | 89.7        | <b>141</b> | <b>191</b> |

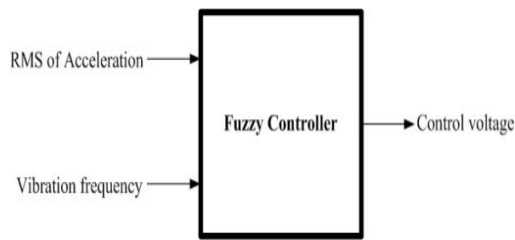


Fig. 8 The structure of the proposed fuzzy controller

The acceleration is measured by the accelerometer (PCB 333B32) and then the signal is amplified through the signal amplifier (PCB 480B02) and transferred to the A/D module NI 9234 on the real-time embedded controller (cRIO-9074). According to the look-up table in Tables II and III, the optimal fuzzy rules can be determined as shown in Table IV, where the first input is the windowed RMS value of the acceleration and the other input is the vibration frequency of the excitation, which can be obtained using the FFT from the acceleration signal. For the two inputs, there are six membership functions, which involves of SS (extreme small), VS (very small), S (small), M (medium), B (big), and VB (very big) as shown in Figs. 9, 10. For the control output of the fuzzy controller, there are six membership functions as shown in Fig. 11, where the larger number means the larger electric field to the ERF TVA. Therefore, the control output of the fuzzy controller is produced using D/A module NI 9263 and this signal is amplified through the high voltage power amplifier (Trek 609A) to control the stiffness of the TVA to suppress the vibration of the main structure. Fig. 12 shows the input-output mapping relation of the proposed fuzzy controller. Fig. 13 shows the designed LabView code which is embedded in the cRIO-9074, where the A/O port is the acceleration signal after amplifying by PCB 480B02 and the AO1 is the control signal transferred to the high voltage amplifier (Trek 609A) to actuate the ERF TVA. Fig. 14 shows the experimental photograph for the ERF TVA testing setup.

TABLE IV

FUZZY RULE OF THE SEMI-ACTIVE CONTROLLER FOR THE ERF TVA

| $f$ | $a_{rms}$ | SS | VS | S  | M  | B  | VB |
|-----|-----------|----|----|----|----|----|----|
| SS  | VS        | VS | Z  | Z  | Z  | Z  | Z  |
| VS  | VS        | VS | S  | Z  | Z  | Z  | Z  |
| S   | VS        | S  | S  | M  | Z  | Z  | Z  |
| M   | B         | VB | M  | S  | S  | Z  | Z  |
| B   | Z         | VB | M  | S  | S  | Z  | Z  |
| VB  | Z         | Z  | VB | VB | VB | VB | VB |

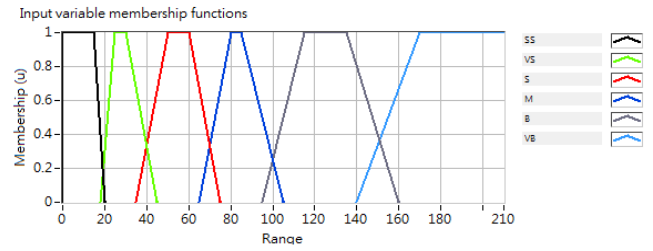


Fig. 9 Membership functions for the first input

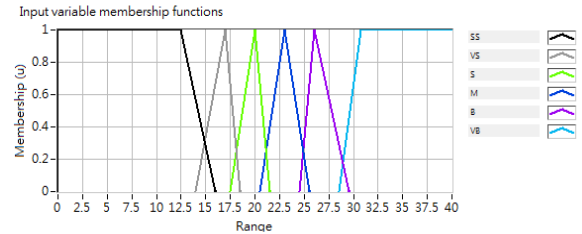


Fig. 10 Membership functions for the second input

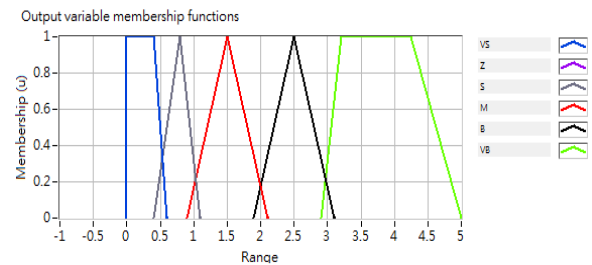


Fig. 11 The membership functions for the output

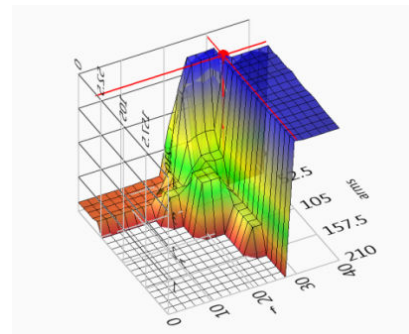


Fig. 12 The input-output mapping relation of the fuzzy controller

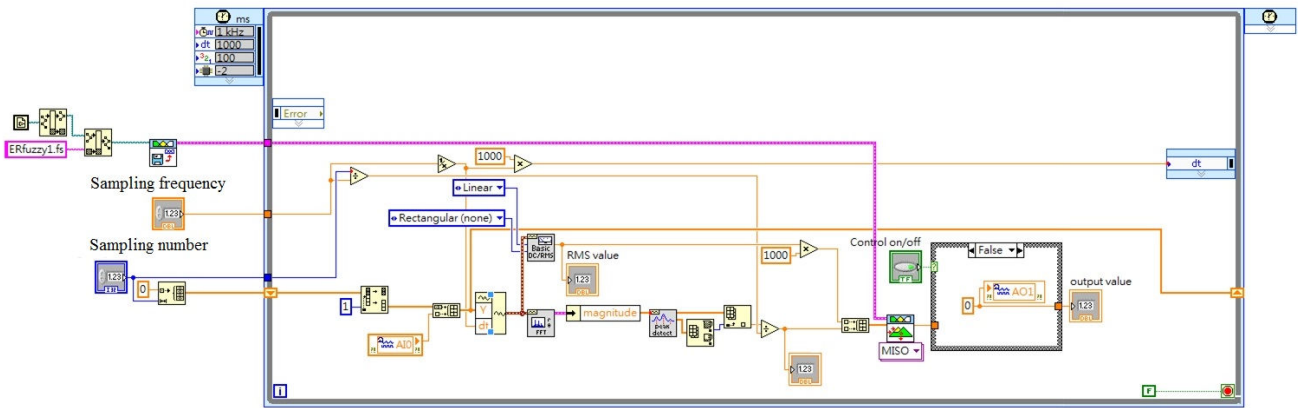


Fig. 13 The embedded LabView Code



Fig. 14The experimental photograph for the ERF TVA testing setup

IV. EXPERIMENTAL RESULTS AND DISCUSSION

The excitation signals at the frequencies from 10 to 70 Hz are inputted to the shaker to make the structure vibrate and Figs. 15-18 shows the comparisons between the responses of no control and the ones of the fuzzy controller at the frequency of 11, 23, 47, and 61 Hz, where the fuzzy controller is turned on at almost 4~5 second. Based on the experimental results, Figs. 17-19 show that the proposed fuzzy controller has the best reduction for the amplitude (about 49%) among the bandwidth of 10~70 Hz. the ERF TVA shows good vibration suppression at the frequencies between 30 and 50 Hz. The worst reduction for the vibration appears at the frequency of 13Hz. Fig. 17 shows that the performance of the semi-active fuzzy controller depends on the excitation's frequencies, because the damping dynamic of ERF is very nonlinear as shown in Fig. 7.

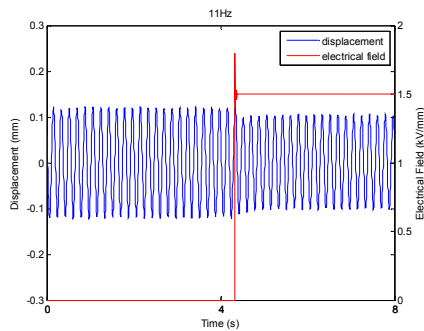


Fig. 15Response using the fuzzy controller at 11 Hz (Turn on at 4.5 sec.)

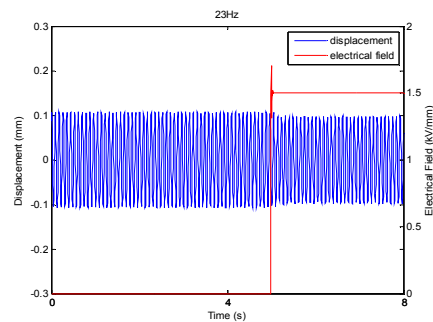


Fig. 16Response using the fuzzy controller at 23 Hz (Turn on at 5 sec.)

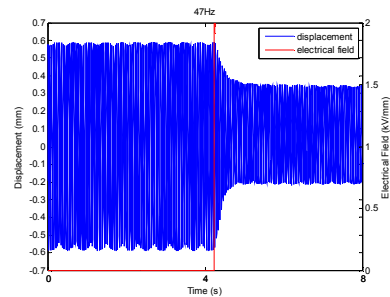


Fig. 17Response using the fuzzy controller at 47 Hz (Turn on at 4.2 sec.)

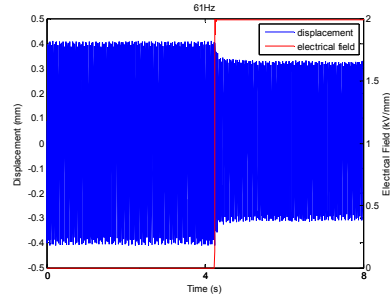


Fig. 18Response using the fuzzy controller at 61 Hz (Turn on at 4.2 sec.)

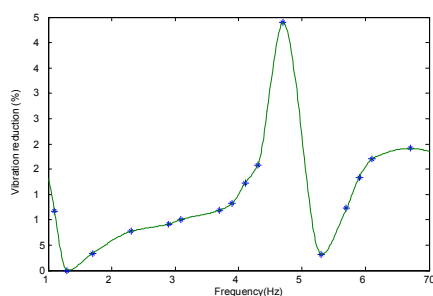


Fig. 19 Vibration suppression rate at the frequencies from 10-70 Hz

## V. CONCLUSIONS

A semi-active fuzzy controller using an ERFTVA is presented for the structure's vibration reduction. Because the nonlinear damping characteristics of the ERF damper needs a look-up table of system parameters for the application with various amplitudes and frequencies, a semi-active fuzzy controller is proposed. For the proposed semi-active fuzzy controller, the fuzzy rules are determined using the optimal solutions based on the windowed RMS acceleration for specified frequencies and amplitudes. To establish the consistency of the simulation and real-time experimental results, the proposed fuzzy controller is implemented in real time using the NI CompactRIO in four studies. The experimental results thus verified the effectiveness of the proposed controller and the performance of the semi-active fuzzy controller depends on the excitation's frequencies.

## ACKNOWLEDGMENT

The authors would like to thank the National Science Council of the Republic of China, Taiwan, for financially supporting this research under Contract No. NSC101-2221-E-027 -029.

## REFERENCES

- [1] W. M. Winslow, "Induced Fibration of Suspensions," *Journal of Applied Physics*, vol. 20, 1949, pp.1137-1140.
- [2] R. S. Stanway, J. L. Sproston, A. K. El Wahed, "Applications of electro-rheological fluids in vibration control: A survey," *Smart Mater. Struct.*, vol. 5, 1996, pp.464-482.
- [3] M. V. Gandhi, B. S. Thompson, "A new generation of innovative ultra-advanced intelligent composite materials featuring electro-rheological fluids: an experimental investigation," *J. Compos. Mater.*, vol. 23, 1989, pp.1232-1254.
- [4] S. B. Choi, Y. K. Park, M. S. Suh, "Elastodynamic characteristics of hollow cantilever beams containing an electro-rheological fluid: Experimental results," *AIAA J.*, vol. 32, 1992, pp.438-440.
- [5] M. Yalcintas, J. Pl Coulter, D. L. Don, "Structural modeling and optimal control of electro-rheological material based adaptive beams," *Smart Mater. Struct.*, vol. 4, 1995, pp.207-214.
- [6] S. B. Choi, Y. K. Park, C. C. Cheong, "Active vibration control of intelligent composite laminate structures incorporating an electro-rheological fluid," *J. Intell. Mater. Syst. Structures*, vol. 7, 1996, pp.411-419.
- [7] C. D. Rahn, S. Joshi, "Modeling and control of an electro-rheological sandwich beam," *J. Vib. Acoust.*, vol. 120, 1998, pp.221-227.
- [8] K. X. Wei, G. Meng, W. M. Zhang, "Vibration characteristics of a rotating beam filled with electrorheological fluid," *J. Intell. Mater. Syst. Structures*, vol. 18, 2007, pp.1165-1173.
- [9] H. Frahm, "Device for damping vibrations of bodies," US patent no. 989958, 1911, <http://patft.uspto.gov/netahtml/PTO/srchnum.htm>.

- [10] M. J. Brennan, "Some recent developments in adaptivetuned vibration absorbers/neutralizers," *Shock and Vibration*, vol. 13, 2006, pp. 531-543.
- [11] L. Kela, P. Vahaoja, "Recent studies of adaptivetuned vibration absorbers/neutralizers," *AppliedMechanicsReviews*, vol. 62, 2009, pp. 060801-1-060801-9.
- [12] A. K. Ghorbani-Tanha, M. Rahimian, A. Noorzad, "A novel semiactive variable stiffness device and its application in a new semiactive tuned vibration absorber," *J. Engineering Mechanics*, vol. 137, 2011, pp. 390-399.
- [13] C. Y. Lee, C. C. Chen, T. H. Yang, C. J. Lin, "Structural vibration control using a tunable hybrid shape memory material vibration absorber," *J. Intell. Mater. Syst. Structures*, vol. 23, 2012, pp.1725-1734.